3A3 Pump Experiment Short Lab Report

Aalok Patwardhan

Emmanuel College

1 Introduction

Two nominally identical pumps were tested. One used pure water as its operating fluid and the other used a 60%-40% Glycerine-Water solution. The glycerine solution pump was kept running at a constant rotational speed whereas for the water pump the impeller speed and throttle opening was varied throughout the experiment.

2 Determination of ratio of viscosity

Dynamic viscosity is proportional to $T\rho/\mathrm{L}$ where T is the time taken for a given volume to pass down the tube, ρ is the density of the liquid and L is the length of the tube. The ratio was calculated to be 12.94, and is tabulated in Table 1.

	Time to drop 4cm, T (s)	**Length of Tube L (m)**	**Fluid Density (kg/m³)**	**Ratio of densities**
Water	33	10	1000	
Glycerine Solution	73	2	1170	**12.941**

Table 1: Calculating ratio of densities

3 Procedure

For the water pump, the fluid was throttled at the outlet at full speed (roughly 49.5Hz) and then the process was repeated for half speed. The experiment was performed again but this time the inlet to the pump was throttled. Finally the glycerine pump was tested keeping the speed at roughly 49.5Hz whilst throttling the outlet.
Using equation 1 calibrated mass flow rate was obtained. The flow rates Q and the pressure rises across the pump was calculated and measured, and non-dimensionalised as in equations 2 and 3 where N and D are the rotational speed and diameter of the impeller respectively. Graphs for all five tests are given in Appendix A.

$$\dot{m} = 0.193\sqrt{\Delta p_{vent}} \tag{1}$$

$$C_Q = \frac{Q}{ND^3} \tag{2}$$

$$C_p = \frac{\Delta p}{\rho N^2 D^2} \tag{3}$$

4 Analysis and Discussion

4.1

Table 2 shows the measured values for inlet and outlet angles and radii of the impeller vanes, as well as the height of the blades.

	Radius (m)	Angle (°)	Height (m)
Inlet Vane	0.013	59	0.0045
Outlet Vane	0.039	46	0.0045

Table 2: Impeller dimensions

The rotor rotates anti-clockwise, doing work on the fluid so that its angular momentum about the centre of the rotor increases. The convex surface of each vane exerts a torque on the fluid and so the fluid exerts a torque on this surface too due to Newton's third law. High pressure thus results on the convex surface. This is shown in Figure 1.

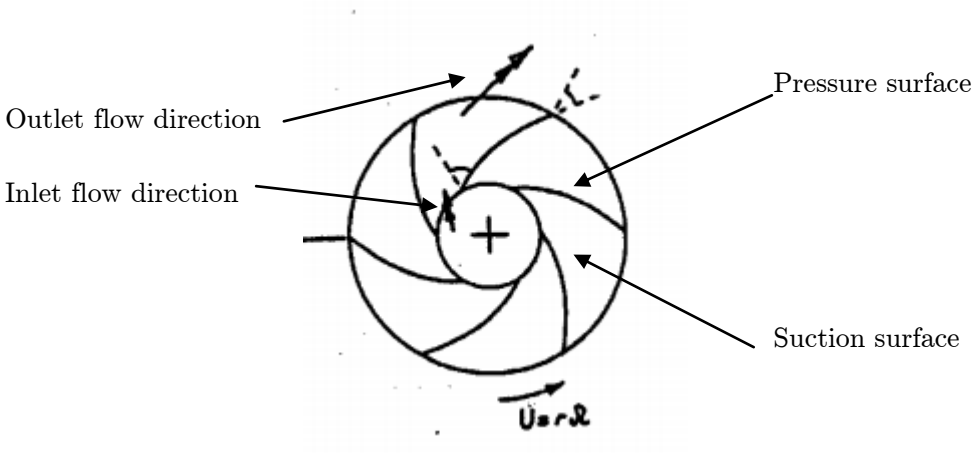

Figure 1: Impeller sketch

4.2 Pump Reynolds Number

The radial velocity at inlet to the vane at maximum flow condition was found by using the mass flow rate of 0.0969kg/m^3 and impeller dimensions, and had a value of $V_{r,in}$=2.98ms^{-1}. Since the tangential velocity was U = N x $V_{r,in}$ = 3.99ms^{-1}, the velocity triangle in figure 2 shows that the relative velocity at the inlet to the vane is V_{rel} = 4.98ms^{-1}. Thus the Reynolds number based on this velocity and the impeller diameter was calculated to be 1.29 x 10^5.

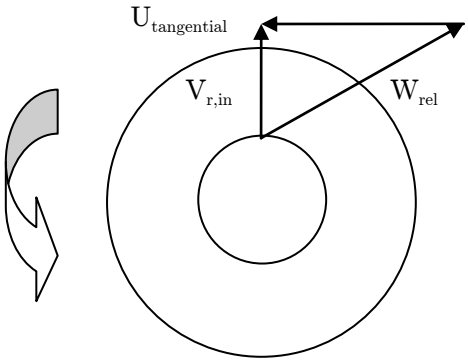

Figure 2

4.3 Dimensionless Cavitation Number

When the local static pressure P_{in} decreases to below the saturation vapour pressure P_v cavitation can be seen to occur. The cavitation pressure can be non-dimensionalised as in equation 4.

$$C_{cav} = \frac{p_{in} - p_v}{\rho N^2 D^2} \tag{4}$$

Cavitation should occur when the above value falls below zero but our measured values of P_{in} are larger because other factors such as streamline curvature pressure losses are not taken into account. We have also assumed that the temperature and therefore $P_{v,sat}$ has stayed the same throughout the experiment which is not the case.
An estimate for the inlet pressure P_{in} was obtained and with the knowledge that the discharge was at atmospheric pressure, and taking into consideration the loss in pressure head between the discharge and the pump delivery, dimensionless cavitation pressure was plotted. This is shown in Appendix B.

For the full speed cases C_{cav} was much lower than for the half speed experiments. This is because the rotational speed N is much larger for the same P_{in}. In general the Inlet cases had a lower P_{cav} than the Outlet throttling cases.

4.4 Performance Curves

The graphs for the five tests are presented in Appendix A.
There was a drop in pressure as the inlet was throttled, and cavitation started roughly when the pressure drop was around 67kPa, corresponding to a C_{cav} less than 0.058. Small vapour bubbles were forming and then bursting quickly initially. As the pressure drop decreased further, large bubbles and splashing was observed near the leading edge of the impeller blades. This is shown in figure 3.

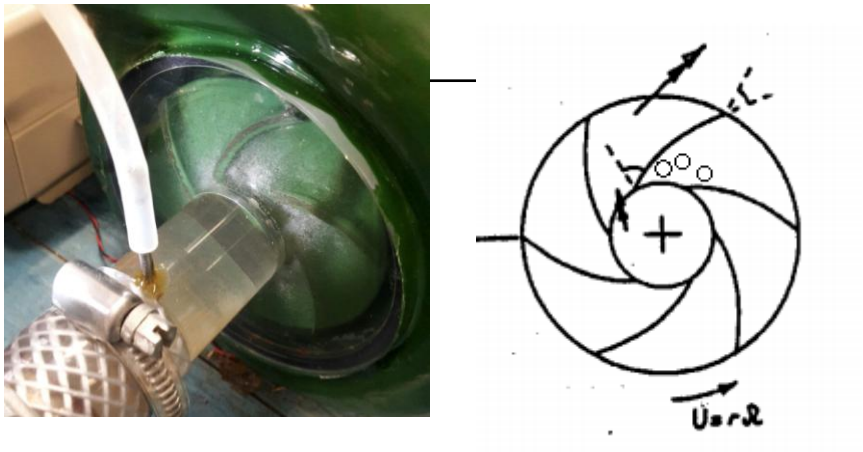

Figure 3

Static pressure increases as the flow diverges from inlet to exit because the velocity relative to the impeller decreases. This is discussed in section 4.6. However the pressure also increases as the flow moves through the rotating impeller and the radius increases, therefore the lowest pressure must be at the impeller blade leading edge. This is corroborated by the streamline curvature as the flow goes from axial to radial sharply.

4.5 Differences in Results (Inlet v Outlet Throttling)

Since the pressure rises across the pump, the inlet pressure is much lower than the outlet pressure. Throttling the inlet can therefore cause cavitation because the local static pressure reduces to less than the saturation vapour pressure.
Although throttling the outlet also causes decreases in pressure, cavitation should not occur due to the increase in pressure across the pump.

4.6 Comparison of Results with Expectations

The pump increases the pressure of the fluid by doing work on it by using the rotational kinetic energy of the impeller. If flow rate increases keeping all else equal, the pressure rise is less, since there is less work done per unit volume.

From section 4.2 the Reynolds number for water was roughly 1.29×10^5, and as the value of k/d is not known (roughness number) it can be inferred that the flow regime is either in the transition zone or turbulent, since at this point in the graph the skin friction coefficient is independent of Reynolds number. The glycerine solution has a Reynolds number of 1.55×10^4; roughly one order of magnitude lower than for water. Since the friction coefficient is lower for this solution, this would create a lower pressure loss.

Cavitation increased with increasing rotation speed. P_{in} was decreased when inlet flow velocity was increased leading to cavitation. If the flow rate reduces, then all else being equal, only the

radial flow velocity component decreases - the tangential component is unchanged. This leads to the inlet angle of the flow to be decreased, as is shown in figure 4.

Figure 4

4.7 Venturi

The Reynolds number for the glycerine solution is much lower than that of water due to the higher viscosity of the solution. From the momentum integral equation it can be induced that the friction factor for glycerine solution is therefore smaller than for water. This leads to the solution having a greater pressure rise for a given fluid flow rate than water.

5 Conclusion

Cavitation occurred when the inlet was throttled at high impeller speeds, because the local static pressure decreased to less than the saturated vapour pressure.

The impeller did work on the fluid to increase its tangential (rotational) velocity and so the convex side of the blade can be thought of as the high pressure surface, and the convex side the suction surface.

The lowest pressure was at the leading edge of the impeller blade. The glycerine solution exhibited a lower pump pressure rise at a given flow rate due to its viscosity being higher and Reynolds number therefore lower.

Appendix A

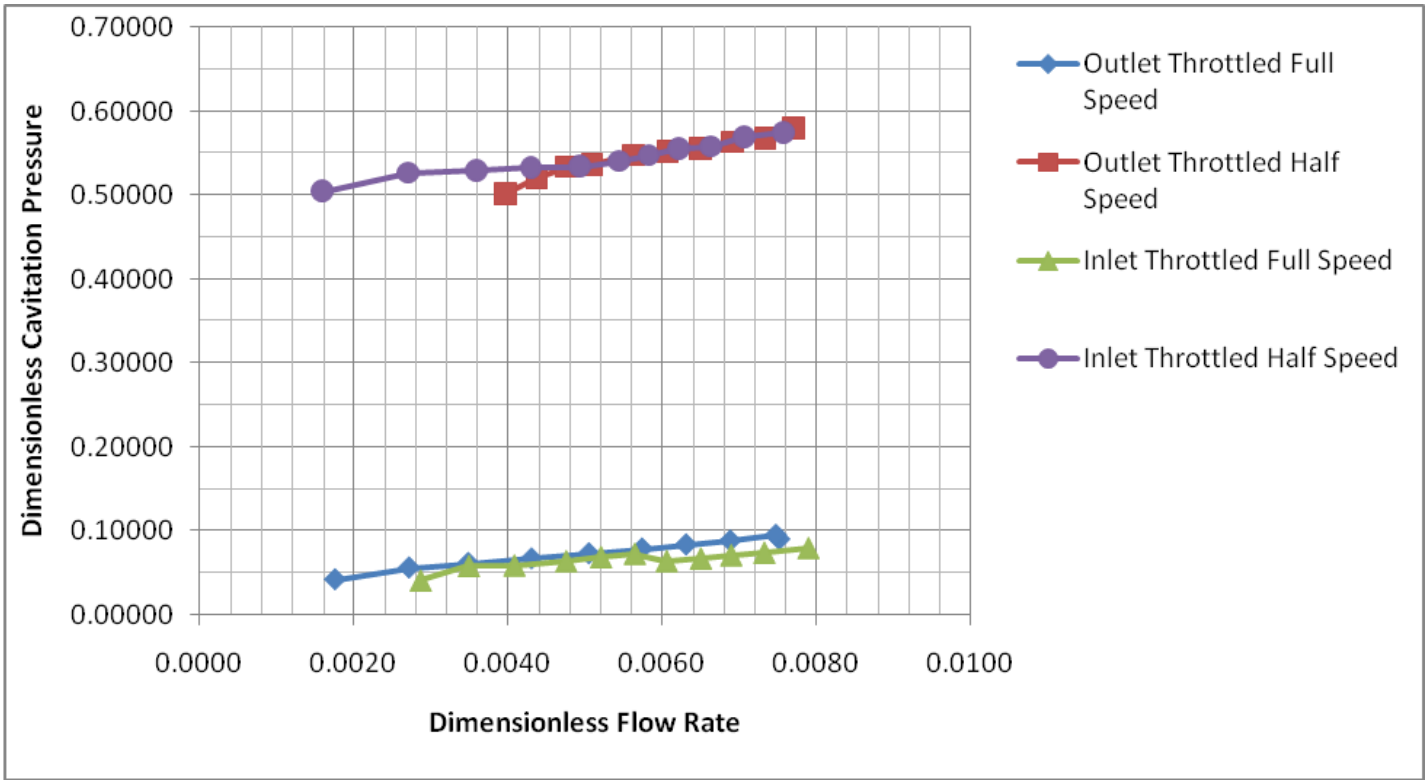

Appendix B